SAND75-0365
Unlimited Release

3151

A Comparison of Mechanical Properties for Several Electrical Spring Contact Alloys

Terry V. Nordstrom

Sandia Laboratories

SF 2900 Q(7-73)

SAND 75-0365
Unlimited Release
Printed June 1976

A COMPARISON OF MECHANICAL PROPERTIES FOR SEVERAL ELECTRICAL SPRING CONTACT ALLOYS*

T. V. Nordstrom
Physical Metallurgy Division
Sandia Laboratories, Albuquerque, New Mexico 87115

ABSTRACT

The major purpose of this work was to determine whether beryllium-nickel alloy 440 had mechanical properties which made it suitable as a substitute for the presently used precious metal contact alloys Paliney 7 and Neyoro G, in certain electrical contact applications. Possible areas of applicability for the alloy were where extremely low contact resistance was not necessary or in components encountering elevated temperatures above those presently seen in weapons applications.

Evaluation of the alloy involved three major experimental areas: 1) measurement of the room temperature microplastic ($\varepsilon \sim 10^{-6}$) and macroplastic ($\varepsilon \sim 10^{-3}$) behavior of alloy 440 in various age hardening conditions, 2) determination of applied stress effects on stress relaxation or contact force loss and 3) measurement of elevated temperature mechanical properties and stress relaxation behavior. Similar measurements were also made on Neyoro G and Paliney 7 for comparison.

The primary results of the study show that beryllium-nickel alloy 440 is from a mechanical properties standpoint, equal or superior to the presently used Paliney 7 and Neyoro G for normal Sandia requirements. For elevated temperature applications, alloy 440 has clearly superior mechanical properties.

---

*This work supported by the U.S. Energy Research and Development Administration.

Table of Contents

Tables

Figures

Figures (cont.)

Figures (cont.)

INTRODUCTION

Electrical spring contact systems in Sandia components employ high strength, high conductivity precious metal base alloys. Because of rapidly rising costs due to price increases for gold and palladium, designers expressed a desire to explore possible non-precious metal base materials which could be substituted at a substantial cost saving. A major constraint placed on selection of any new materials, however, is the requirement that contact resistance be low enough that precious metal plating of the contact is unnecessary. Problems with obtaining consistently high quality plating products from suppliers caused this restraint. A second reason for interest in improved contact materials is that some new initiatives programs are relying upon components for high temperature operation where contact materials with elevated temperature mechanical stability superior to present materials are needed.

The general requirements of high strength and reasonable conductivity limited the number of candidate materials significantly. The requirement for no plating further limited the selection. Nickel-base alloys appeared to be the principal group of materials which might fill all the qualifications. Work by R. E. Cuthrell[1,2] has confirmed the relatively low contact resistance in the unplated condition for nickel alloys.

One of the most attractive alloys from the standpoint of strength and conductivity is beryllium-nickel Alloy 440.Ⓣ It is a nickel-1.95 wt.% beryllium, 0.50 wt.% titanium alloy. Typical properties for the alloy are given in Table I[3] along with comparative properties for Neyoro G and Paliney 7,[4] the two alloys presently used in spring contacts. Note that

---

Ⓣ Kawecki-Berylco Industries, Reading, PA.

TABLE 1

Minimum Reported Properties for Three Contact Alloys

	Be-Ni Alloy 440		Ptliney 7	Neyoro G	
	Condition AT	Condition HT	Heat Treated	Condition AT	Condition HT
Conductivity % IACS	7%	NA	5.4	12.2	12.2
Modulus of Elasticity (PSI)	27×10^6 (186 GPa)	27×10^6 (186 GPa)	17×10^6 (117 GPa)	16×10^6 (110 GPa)	16×10^6 (110 GPa)
Yield Strength (0.2% offset) (PSI)	150,000 (1.03 GPa)	230,000 (1.58 GPa)	110,000 (0.75 GPa)	95,000 (0.65 GPa)	NA
Tensile Strength (PSI)	215,000 (1.46 GPa)	270,000 (1.86 GPa)	165,000 (1.15 GPa)	135,000 (.93 GPa)	150,000 (1.03 GPa)
Elongation (pct)	12	8	2	7	2
Fatigue Strength (10^7 - 10^8 cycles) (T = 25°C)	NA	95,000 (.65 GPa)	50,000 (.34 GPa)	NA	30,000 (.21 GPa)

alloy 440 is equal or superior in all pertinent properties. Alloy 440 can be strengthened both by cold-working and age-hardening. While general mechanical properties are available from the manufacturer for alloy 440, neither microdeformation, stress relaxation behavior nor the temperature dependence of mechanical properties for the alloy are well established. All of these properties are important for using any material with confidence in a spring contact where long term storage under stress is common.

Experiments were devised to measure properties related to three main areas; aging studies, applied stress response and storage temperature effects. Each will be described in turn.

1) Aging studies: samples of Be-Ni alloy 440 were aged for times ranging from 15 to 240 minutes (supplier recommended time, 90 minutes) at 510°C. Subsequently, the microplastic ($\epsilon \sim 10^{-6}$ plastic) and macroplastic ($\epsilon \sim 10^{-3}$ plastic) deformation behavior of the samples were measured. These tests were performed in order to evaluate the kinetics of the development of microyield strength. Microdeformation behavior is important to spring contact behavior but if it is possible to use macroplastic behavior to evaluate spring materials, then experimental problems would be eased considerably. The precision required to perform microdeformation experiments makes them very tedious and time consuming.

2) Applied stress effects: relatively long term room temperature tensile stress relaxation experiments were performed on Be-Ni alloy 440 in the standard age hardened conditions at an initial stress of 200 KSI (1.38 GPa). Also, short term stress relaxation tests were performed over the range of 150-240 KSI (1.03-1.65 GPa) initial stresses. The results of the relaxation tests are compared to earlier results for Neyoro G and Paliney 7. With these experiments, it was hoped that the resistance of

the alloy to contact force loss during long term storage under stress could be evaluated.

3) Test temperature effects: relatively long term tensile relaxation experiments were performed at 200°C on the 440 alloy, Neyoro G and Paliney 7. The 440 alloy was tested at an initial stress of 150 KSI (1.03 GPa) and the two Ney alloys were tested at an initial stress of 100 KSI (690 MPa). This is due to the lower overall strength of the Ney alloys as shown in Table I. Also, tensile test measurements were made of the proportional limit, (P.L.); 0.2% offset yield strength, (σ_y), and ultimate tensile strength, (σ_{UTS}), for all three alloys over the temperature range -196°C to 200°C. These measurements were all directed at establishing the merits of the three alloys relative to mechanical stability in an elevated temperature environment.

EXPERIMENTAL PROCEDURE

Beryllium-nickel alloy 440 strip was obtained from Kawecki-Berylco Industries. The material was 0.040" (1 mm) thick by 1" (25.4 mm) wide and was in both the solution annealed and quenched condition (condition A) and in the solution annealed, quenched and cold-worked 40% condition (condition H). The chemical composition is presented in Table II. Standard tensile samples were machined with a gage section of 0.25" (6.35 mm) by 0.040" (1 mm) and gage length of 1.50" (38 mm). All age hardening heat treatments were performed in a forming gas atmosphere (93% N_2, 7% H_2) to reduce oxidation of the samples. Temperature was controlled over the length of the sample to better than ±2°C. Specific details of the procedures followed in the mechanical testing are presented in the following three sections.

TABLE II

Composition of Beryllium-Nickel Alloys

	Be	Fe	Si	Al	B	C	Pb	Ti	Cr	Mg	Ni
Initial Condition A	1.89	.12	.03	.03	< .001	.027	.001	.47	.06	.003	Bal.
Initial Condition B	1.90	.12	.06	.10	< .001	.058	.001	.46	.04	.006	Bal.

1) Microdeformation Experiments: The details of the microdeformation experiments and the necessary control levels have been outlined in detail elsewhere.[5] High resolution, resistance strain gages are bonded on opposite sides of the sample. Output from the gages is amplified such that a strain resolution of 10^{-7} is obtained, however, the accuracy of the measurement is much lower ($\pm 3 \times 10^{-6}$). The samples are first preloaded a small amount (0 KSI, 69 MPa) then loaded to a higher level of stress and subsequently returned to the base stress. Any change in strain output is measured. The samples are loaded in this fashion to progressively increasing levels of stress. The data is presented as the stress necessary to obtain plastic strains of 10×10^{-6} (10 microstrain) and 100×10^{-6} (100 microstrain).

2) Stress Relaxation Experiments: The room temperature stress relaxation experiments were performed on a closed loop electrohydraulic tensile testing machine operating under strain control. Strain was monitored using a Micromeasurements #EP-08-062AQ-350 strain gage attached to the gage section with Mbond 610 adhesive.* These gages are specifically designed for plastic strain measurements and thus stress relaxations were carried out following plastic strains of up to 9%. The room temperature was constant to within ±3°C. The sample temperature was held to ±1°C by encasing sample and grips in a foam insulating jacket. The tests conducted at 200°C were performed on an Instron machine using constant crosshead displacement. Details of the temperature bath used have been presented in an earlier report.[6] All samples were loaded to the initial stress value at a constant crosshead displacement or strain rate of .02"/min (.5 mm/min).

*Micromeasurements Manufacturing Company, Romulus, Michigan.

3) Tensile Tests: All of the tensile tests were performed on an Instron machine at a constant crosshead displacement of 0.02 in/min (.5 mm/min). Strain was measured using an Instron 1" -10% elevated temperature clip gage, model 351-11A. The tests above room temperature were performed in a resistance heated silicone oil bath. The tests at -50°C were conducted in an alcohol bath cooled by passing liquid nitrogen through a copper coil immersed in the alcohol. For tests at -196°C the specimens were immersed in liquid nitrogen.

RESULTS AND DISCUSSION

The results are organized in the same sequence as presented in the introduction: aging studies, applied stress effects, and test temperature effects.

1) Aging Studies: The effect of aging time at 510°C on deformation resistance is shown in Figures 1 and 2. The behavior is typical of age hardening systems with the strength rising rapidly at short aging times then falling at longer aging times. The standard aging treatment for the solution annealed material is 90-minutes at 510°C. Figure 1 shows that this time corresponds to the maximum strength for the commonly measured values of the 0.2% offset yield strength and ultimate tensile strength. For the micro-yield properties measured in the present study, Figure 1 indicates that over-aging, and a consequent slight reduction in the microdeformation resistance, begins at times of 90 minutes and more. The effect is small, however, and probably would not significantly affect the spring properties of the alloy.

For the cold-worked and aged material there is also an over-aging and weakening behavior for the microdeformation properties whereas the macrodeformation resistance begins to decrease only for the longest aging times.

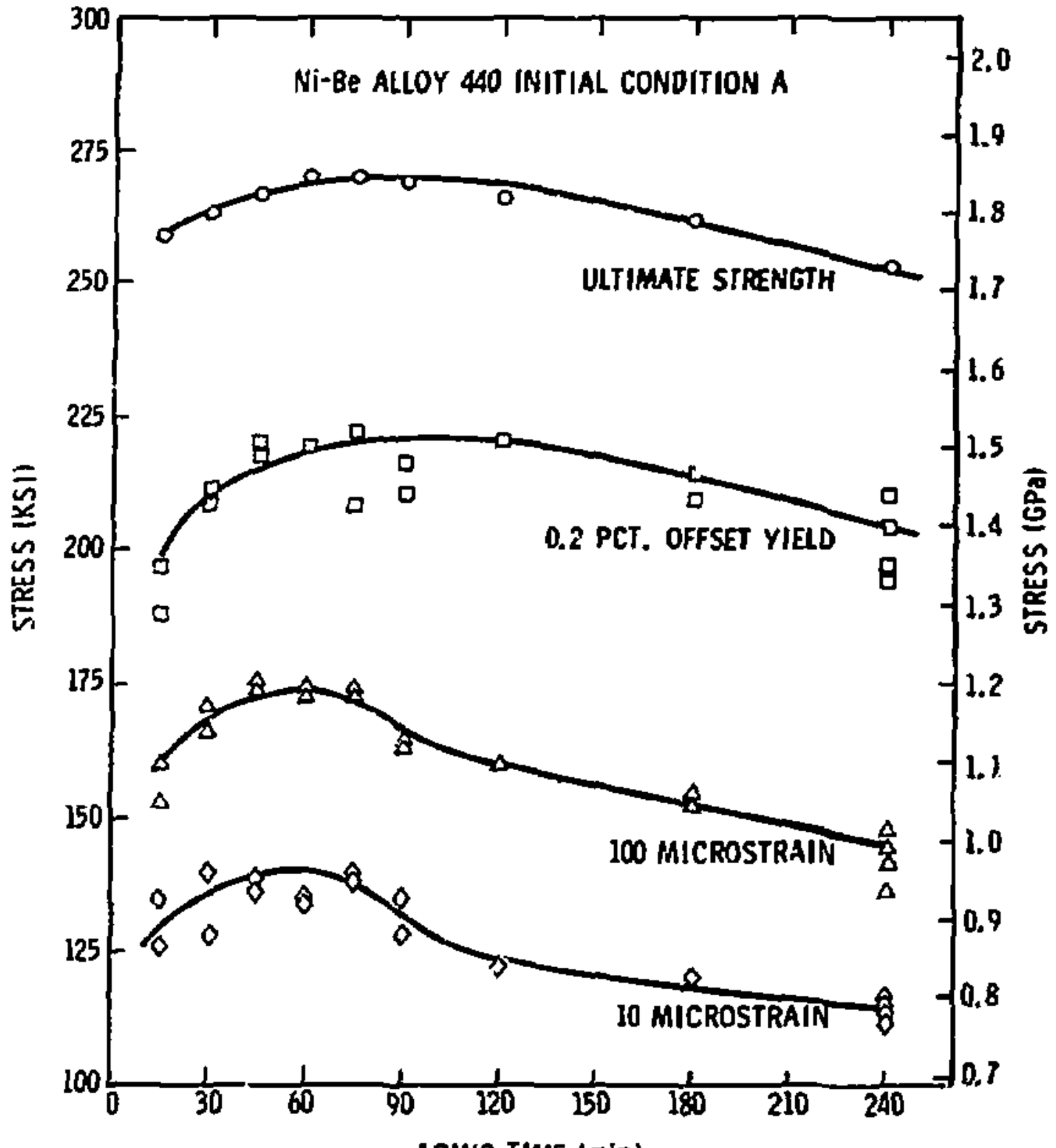

Figure 1: The effect of aging time at 510°C on the room temperature mechanical properties of beryllium-nickel alloy 440, initial condition A.

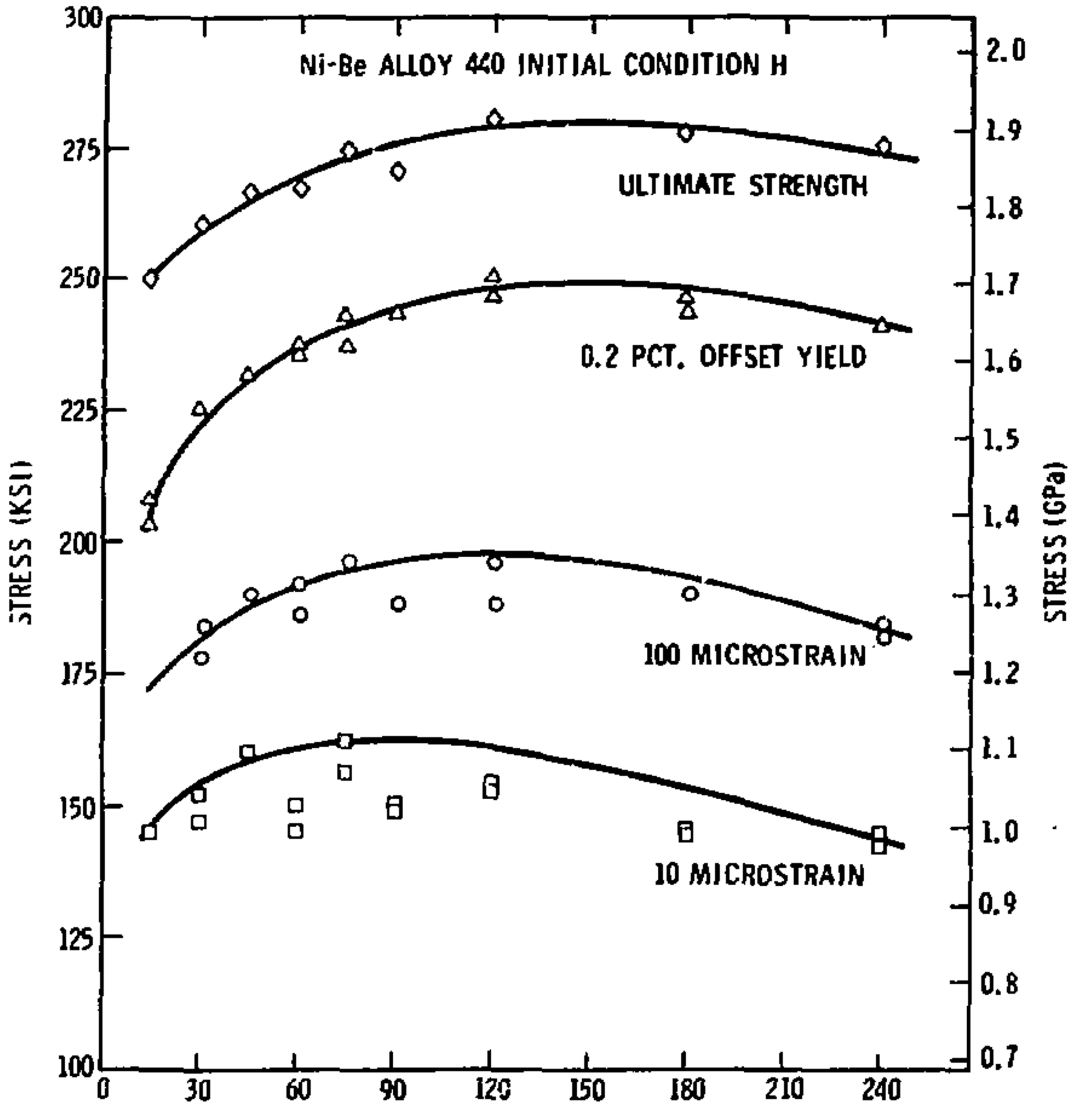

Figure 2: The effect of aging time at 510°C on the room temperature mechanical properties of beryllium-nickel alloy 440, initial condition H.

Again, the standard 90-minute age is probably the most suitable for an optimum strength behavior.

Transmission electron microscopy and scanning electron fractography investigations were performed to ascertain a cause of the more rapid decrease in microdeformation properties in comparison to macrodeformation properties with overaging. Transmission foils of the solution annealed and standard 90-minute aged material were examined. Representative structures are shown in Figures 3 and 4. The interior region of grains has the "tweady" structure seen in Figure 3. This corresponds to the aging behavior previously reported by German investigators.(7) However, in regions adjacent to grain boundaries, as Figure 4 shows, the precipitation reaction is discontinuous. Apparently, enhanced diffusion or nucleation near grain boundaries is allowing precipitation of the stable γ phase NiBe.(7)

That this structure near boundaries is weaker than the grain interior structure is indicated by the scanning electron fractography pictures in Figure 5. At low magnification the fracture surface appears as a typical brittle intergranular failure mode with very little ductility in the material, Figure 5a. However, when the magnification is increased, a dimple rupture type structure is seen to be imposed on the intergranular failure mode, Figure 5b. These dimple ruptures indicate a ductile failure. These observations can be interpreted as meaning that failure has occurred in the localized, relatively soft grain boundary phases by microvoid formation around the large γ particles in this region.

The proportion of the structure transformed to this lower strength phase increases with aging time. This increased fraction of low strength phase accounts for the more rapid over-aging of the micro-yield properties for the following reason: It is generally believed that the onset of

Figure 3: Transmission electron micrograph of the grain interior structure of beryllium-nickel alloy 440, condition AT.

Figure 4: Transmission electron micrograph of structure at a grain boundary for beryllium-nickel alloy 440, condition AT.

(a) 63X

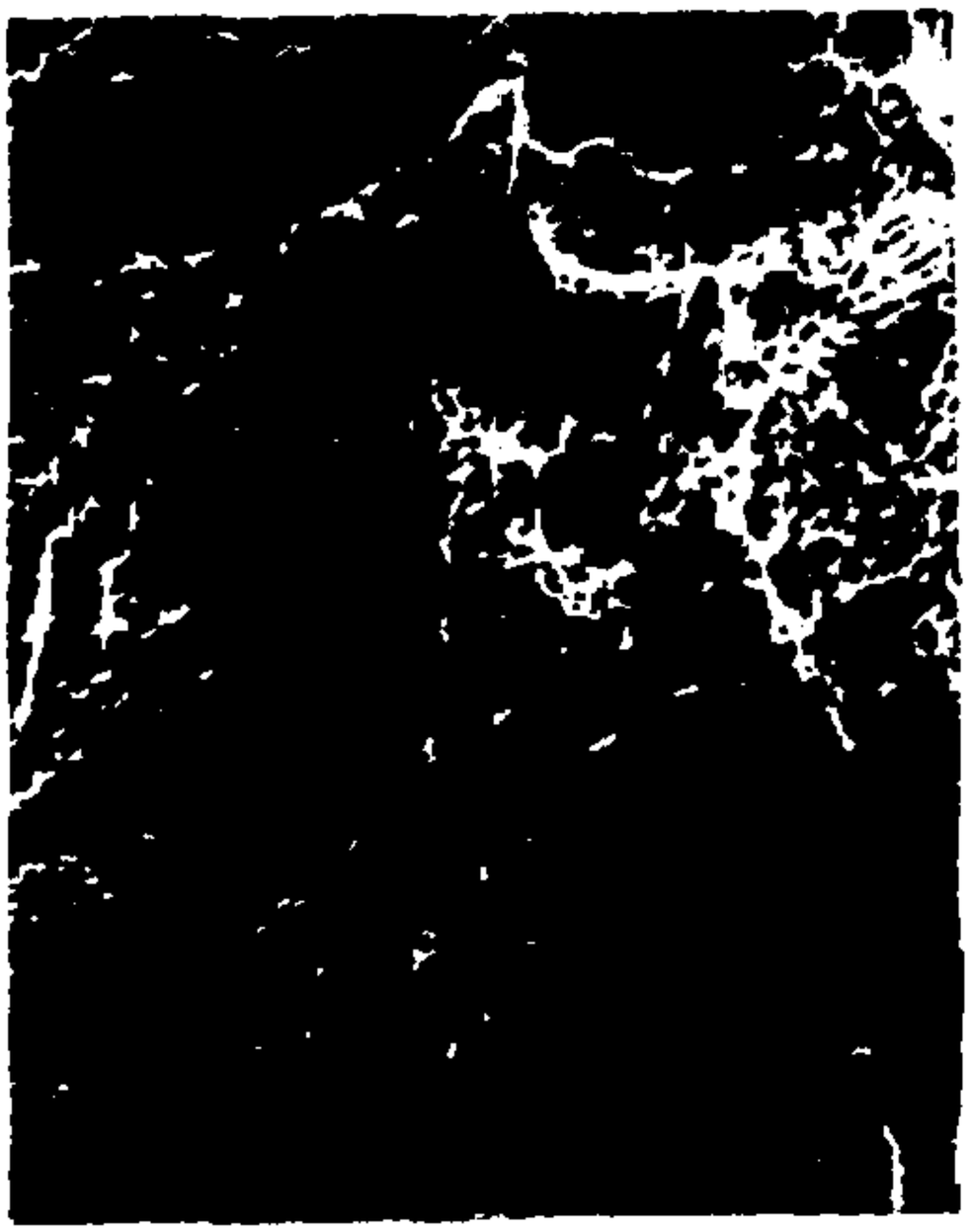

(b) 630X

Figure 5: Scanning electron micrographs of the fracture surface of a beryllium-nickel alloy 440 sample, initial condition AT.

plastic deformation occurs at grain boundaries through grain boundary sliding and the increasing amount of the lower strength phase would allow greater deformation near boundaries at a lower stress. The macro-yield value does not drop as rapidly due to the fact that slip will probably occur throughout the grains during macrodeformation. The high strength phase of the grain interiors should not weaken significantly with the increased aging times studied in this work since electron diffraction shows no significant change of structure, even for the longest aging times studied.

No studies of the effect of aging on stress relaxation behavior were made. This was due to the observation that times for peak strengths relative to both micro- and macro-yield are approximately equal. Treatments other than the standard aging would probably not give significantly improved stress relaxation resistance when account is taken of the level of temperature and time control achieved by commercial heat treaters.

2) Effects of Applied Stress on Stress Relaxation: The effect of initial applied stress on the relaxation behavior was studied at room temperature over the range of 150 KSI (1.03 GPa) to 242 KSI (1.65 GPa). Before presenting the results, an outline is given of the type of model that is generally employed to characterize stress relaxation or transient creep in the temperature region of less than one-third the absolute melting temperature. Recovery can be discounted as a significant contribution to the creep process in this temperature regime.

A model can be constructed to accurately describe in parametric terms the behavior of a material during stress relaxation. Generally it is assumed that deformation occurs by stress-assisted thermal activation of dislocation segments. Stress relaxation is, in fact, plastic deformation through the simple relation,

$$\dot{\sigma} = \dot{\epsilon}_p E \qquad (1)$$

where $\dot{\epsilon}_p$ is the plastic strain rate, $\dot{\sigma}$ is the measured stress relaxation rate and E is Young's Modulus. When crosshead position control is used (conventional Instron tests), the machine stiffness has a significant effect on the amount of strain that is occurring and must be taken into account in Eq. (1), by changing the effective modulus.

The solid is divided into subvolumes of a length L on a side. The area L^2 is the minimum area a dislocation will sweep out and not return to its previous position. If σ is the applied stress and σ_i is some long-range back stress resisting motion of the dislocation and not surmountable by thermal activation, then the additional energy which must be supplied in sweeping the dislocation of length L across a distance L is

$$W = U + \bar{b}L^2(\sigma_i - \sigma) \approx U - \bar{b}L^2\sigma_e \quad . \qquad (2)$$

Here U is the energy required to overcome the resistance to deformation due to the short-range hardening mechanism, σ_e is the effective stress acting to aid the overcoming of the short-range barrier and $\bar{b}$ is the burger's vector. The precise nature of the barrier in the Ni-Be alloy is not known, but is probably the cutting of a dislocation through a precipitate particle. During stress relaxation, the long-range hardening stress can be increased due to strain hardening so that

$$\sigma_e = \sigma_e^o - H\epsilon_p \qquad (3)$$

where ϵ_p is plastic strain and σ_e^o is the effective stress at the start of a relaxation. It is assumed that H, the work-hardening rate during a relaxation, is equal to the slope of the stress-strain curve just prior to

the start of the relaxation. This assumption is reasonable since the flow stress of Li-Be is not particularly strain rate sensitive.

The decrease in applied stress during the relaxation also reduces the effective stress. Thus, the effective stress during a relaxation varies as

$$\sigma_e = \sigma_e^o - \epsilon_p(H + E) \tag{4}$$

According to rate theory, the probability that a given dislocation segment will be thermally activated over a barrier in unit time is ν' exp-(W/kT). ν' is a vibrational frequency of the dislocation ($\nu' \approx 10^{10}$ to 10^{11}/sec). The strain produced per unit volume by one dislocation segment moving is approximately $\bar{b}L^2$. An equation for strain rate during relaxation can thus be formulated as

$$\dot{\epsilon} = \frac{\nu \bar{b} L^2}{L^3} \exp - W/kT \tag{5}$$

$$\dot{\epsilon} = \frac{\nu \bar{b}}{L} \exp - \left| \frac{U - \bar{b}L^2 \sigma_e^o - \epsilon_p(H + E)}{kT} \right| \tag{6}$$

Integration of this equation with respect to time gives a relation for the strain of $\epsilon_p = A \log (1 + Bt)$ where

$$A = \frac{kT}{\bar{b}L^2 (H + E)} \tag{7}$$

and

$$B = \frac{\nu \bar{b} L^2 (H + E)}{kT} \exp - \left| \frac{U - \bar{b}L^2 \sigma_e^o}{kT} \right| \tag{8}$$

Converting to change in stress during relaxation gives

$$\Delta\sigma = EA \log (1 + Bt) \qquad (9)$$

The results of the stress relaxation experiments are plotted in Figure 6 as percent stress relaxed versus the logarithm of time. In general, all the results for initial stresses ranging from 150 KSI (1.03 GPa) to 242 KSI (1.65 GPa) behave linearly with respect to log time. There is, however, a significant increase in the slope of the curves with increasing applied initial stress.

There are a number of terms in equation 9 that can vary as the initial stress is increased to higher levels. Those possibly varying are U, L, σ_e^o and H. Using data from the present experiments alone, variations in U, L, or σ_e^o cannot be determined with any degree of certainty. However, measured values of H are given in Table III along with the initial strain and predicted relaxations after one year based on extrapolation of the data in Figure 6. In addition, earlier more extensive experiments on beryllium copper alloy 25 have measured changes in the other terms in that structurally very similar material.[9]

Attempts were made to replot the data in Figure 6, normalized to account for the changes in H. Only at very low stresses or high values of H did the correction improve the fit of the data to the model. In beryllium-copper alloy 25, L was shown to decrease with increasing applied stress.[9] This variation correctly accounts for the increased slope of the stress relaxation curves in Figure 6 with applied stress.

The type of model developed here does describe the behavior of beryllium copper for times up to a year.[10] Therefore, the predictions in Table III of long-term room temperature relaxation are based both on previous experimental results and a model which accurately predicts material behavior.

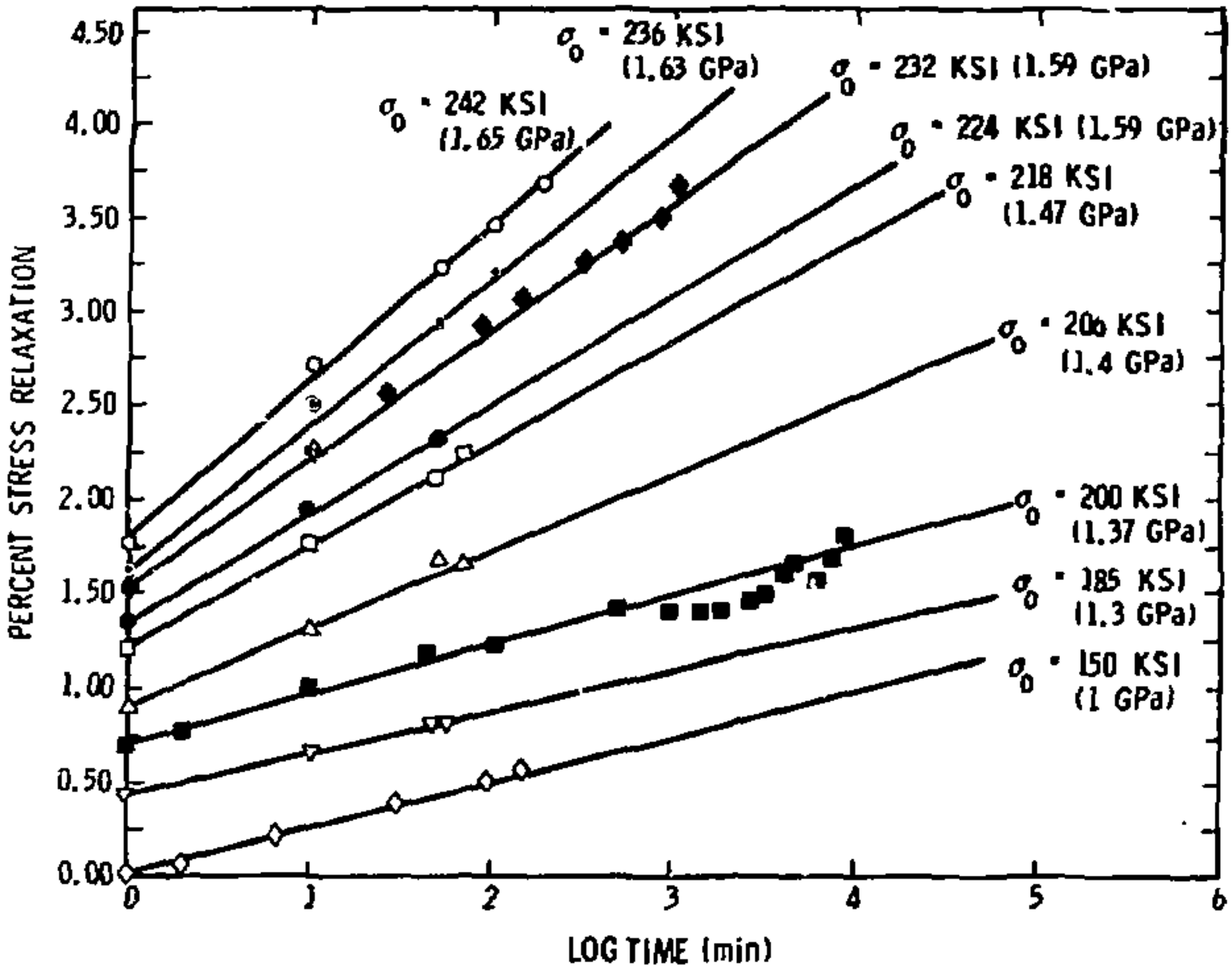

Figure 6: The effect of initial stress on room temperature stress relaxation behavior of beryllium-nickel alloy 440, initial condition AT.

TABLE III

Stress Relaxation Data for Beryllium-Nickel 440
Initial Condition AT

ε_o	σ_o (ksi)	$\Delta\sigma$ (1 year) (psi)	H (psi)
.005	150	2000	3.06×10^7
.00625	180	3000	2.50×10^7
.0075	206	5700	1.25×10^7
.00875	218	9400	7.20×10^6
.010	224	10200	4.37×10^6
.0125	232	12200	2.50×10^6
.0150	236	13500	1.60×10^6
.020	242	15000	1.01×10^6
.025	246	16200	6.40×10^5
3.0	251	17500	3.60×10^5

Figure 7 shows the effect of initial condition on the stress relaxation behavior of alloy 440. The AT material is aged from the fully annealed condition while the HT material is aged from the 40% cold-worked condition. There is very little difference in the rate of relaxation for the materials. The initial stress in both cases is below the nominal yield strength. In this relatively low stress regime it might be assumed that deformation in both conditions is controlled by the same mechanism - probably shearing of precipitates. If deformation in both conditions were controlled by the same mechanism, it would not be surprising that the relaxation rates were approximately equal despite different ...itial conditions. The slightly higher relaxation rate in the HT material may be due to the larger dislocation density initially present.

3) Temperature Effects: Yield Behavior. The effect of temperature on the proportional limit, 0.2% offset yield strength and ultimate tensile strength is shown in Figure 8 for alloy 440 in both the AT and HT conditions. All three variables decrease with increasing temperature at approximately the same rate for both alloy conditions. It is interesting to note that, while the proportional limit and yield strength differ greatly for AT and HT, the difference in ultimate strength for the two conditions is much less marked. In comparison, Figures 9 and 10 present the same data for Neyoro G and Paliney 7, respectively. The strengths of both alloys are considerably lower than the alloy 440. The reduced temperature sensitivity of the macro-yield properties of Neyoro G agrees with our earlier work comparing the temperature dependence of the micro-yield properties for the two alloys.[5] (The strengthening mechanism in Neyoro G is thought to be an order type hardening which may be less sensitive to temperature than precipitate shearing.)

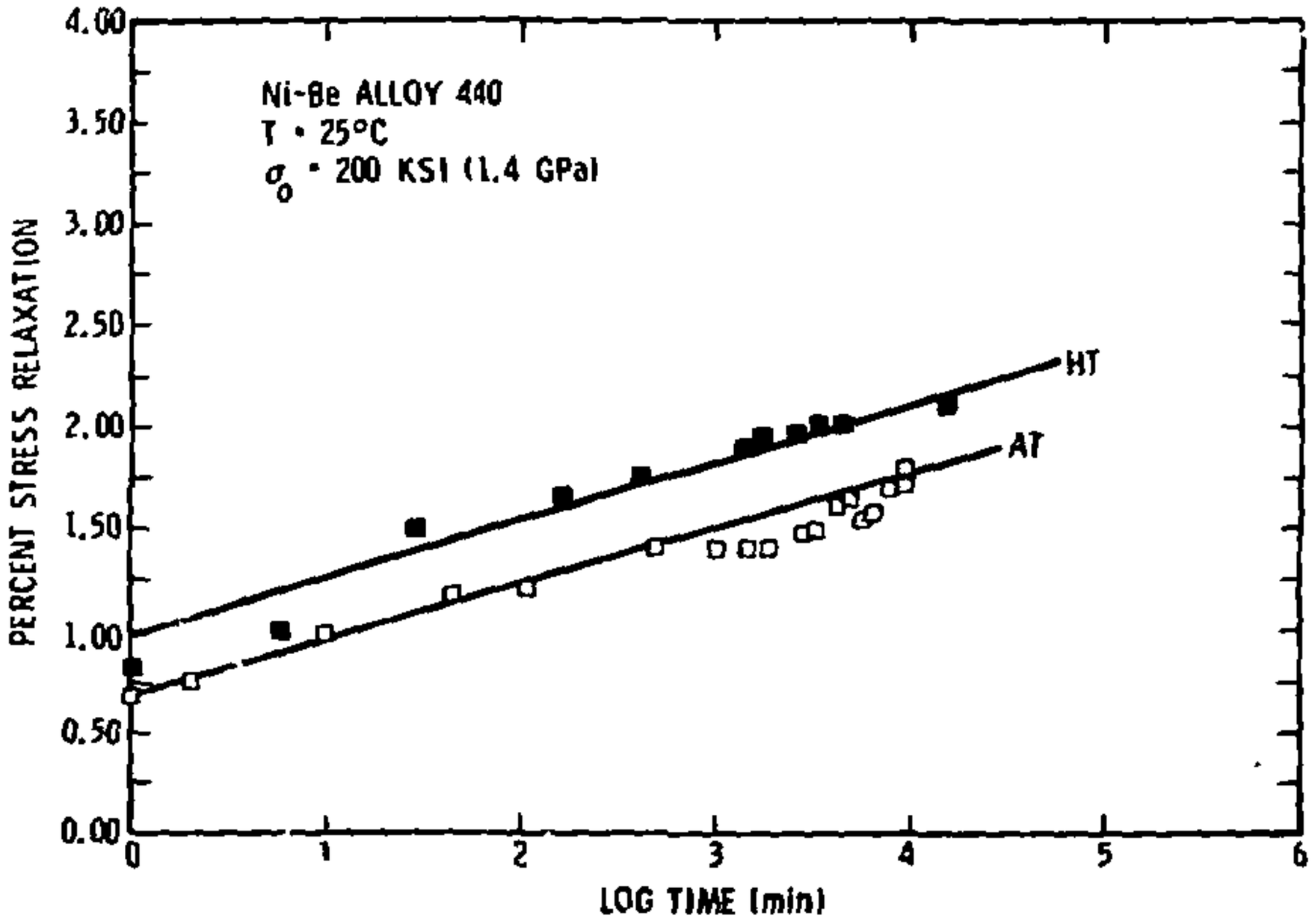

Figure 7: The effect of initial condition on the room temperature stress relaxation behavior of beryllium-nickel alloy 440.

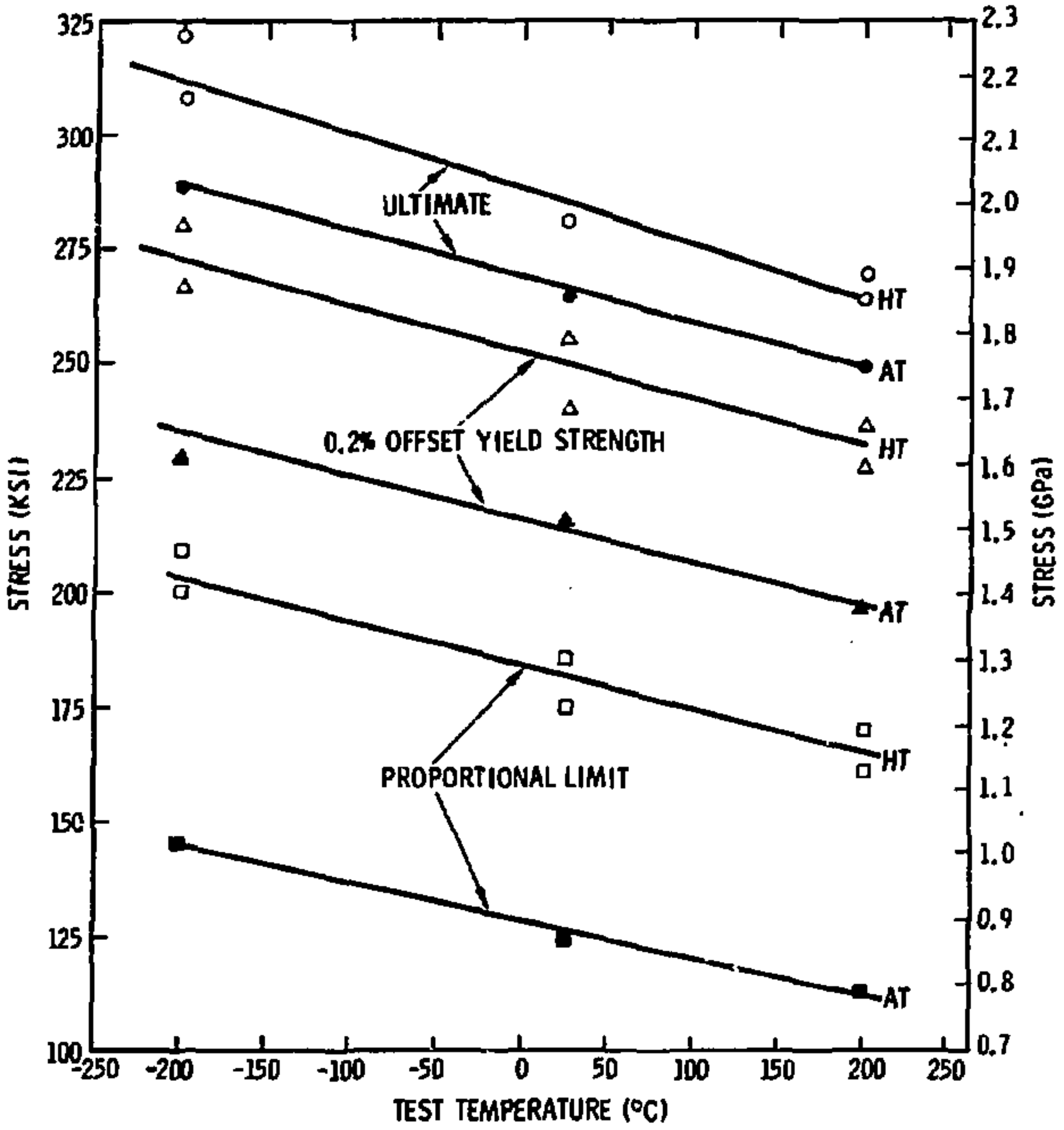

Figure 8: Effect of test temperature on the mechanical properties of beryllium-nickel alloy 440 in both conditions AT and HT.

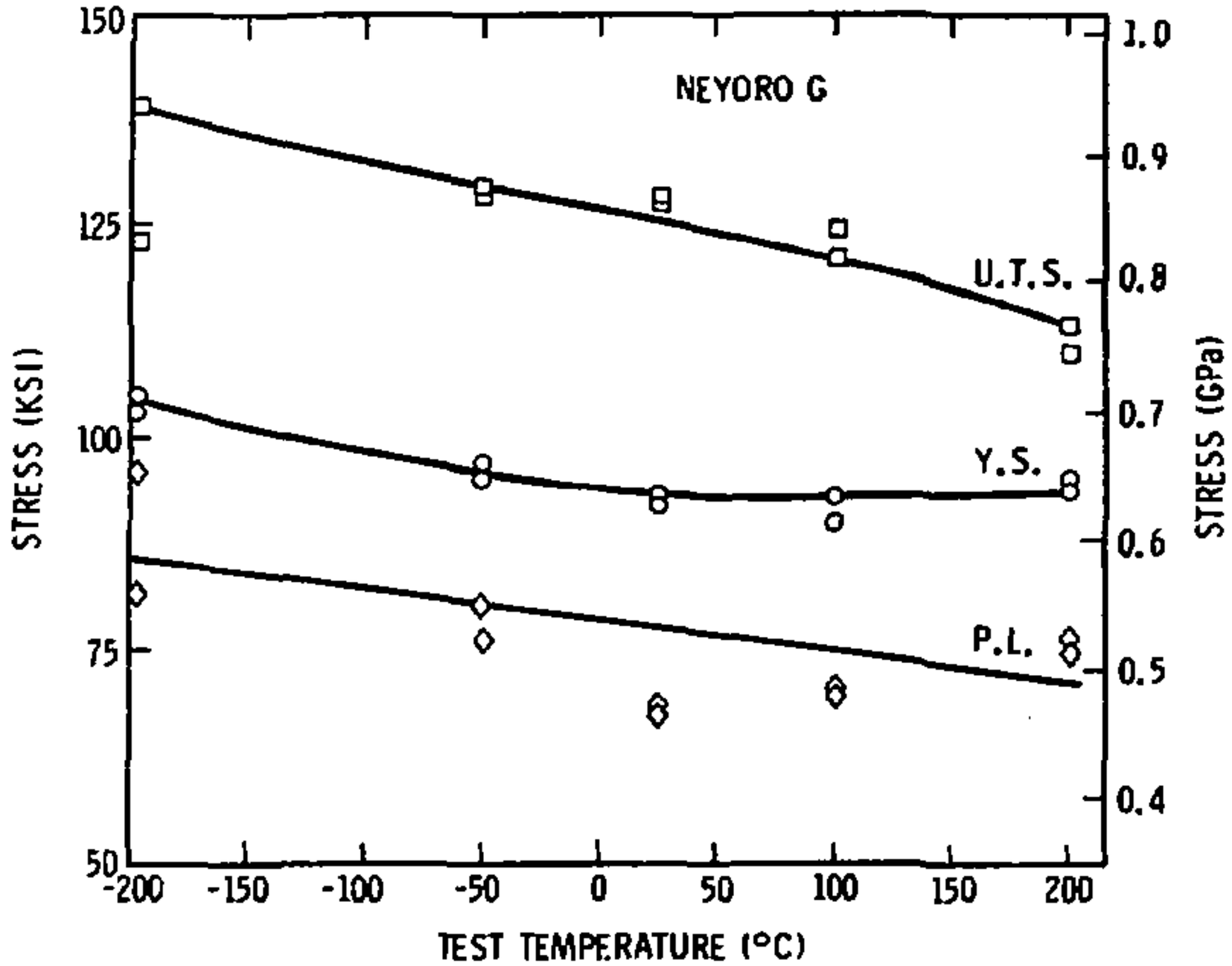

Figure 9: Effect of test temperature on mechanical properties of Neyoro G. Initial condition of Neyoro G samples was solution annealed 10 minutes at 704°C, water quenched, aged 20 minutes at 426°C.

4) Temperature Effects: Stress Relaxation Behavior. The temperature dependence of the stress relaxation behavior of alloy 440 AT is shown in Figure 11. Relaxation is seen both at room temperature and 200°C, though not at a rate that would cause concern for electrical contact design. Extrapolation of the data would predict only a few percent relaxation after years of service. Such an extrapolation is reasonable and prudent since the model presented earlier correctly predicts the increased relaxation rate at elevated temperatures. The test temperature is still low enough that the physical assumptions made in the model remain correct in alloy 440. The fairly large amount of scatter in the results is due to both the relatively small stress changes involved and room temperature fluctuations during test.

In comparison, Figure 12 shows stress relaxation behavior at 200°C for Neyoro G and Paliney 7. Because of these alloys lower relative strength, the tests were performed at 100 KSI (690 MPa) initial stress. The two alloys vary greatly in the amount of stress relaxation with the Neyoro G relaxing about six times as much as the Paliney 7 after 10^4 minutes testing. The Neyoro G does have a slightly lower yield strength at 200°C as shown in Figures 8 and 9. In addition, Neyoro G is a gold base alloy and has a solidus temperature of 930°C whereas Paliney 7 is a Palladium base alloy and has a higher solidus temperature of 1016°C. Models which predict logarithmic stress relaxation behavior as observed in all the alloys at room temperature begin to lose their applicability at temperatures above about 0.3 to 0.4 T_m, where T_m is the absolute melting temperature. The 200°C test temperature is in that range of temperature for both alloys. The apparent deviation from the predicted linear behavior with log time shown by the Neyoro G at 200°C in Figure 12 probably indicates that

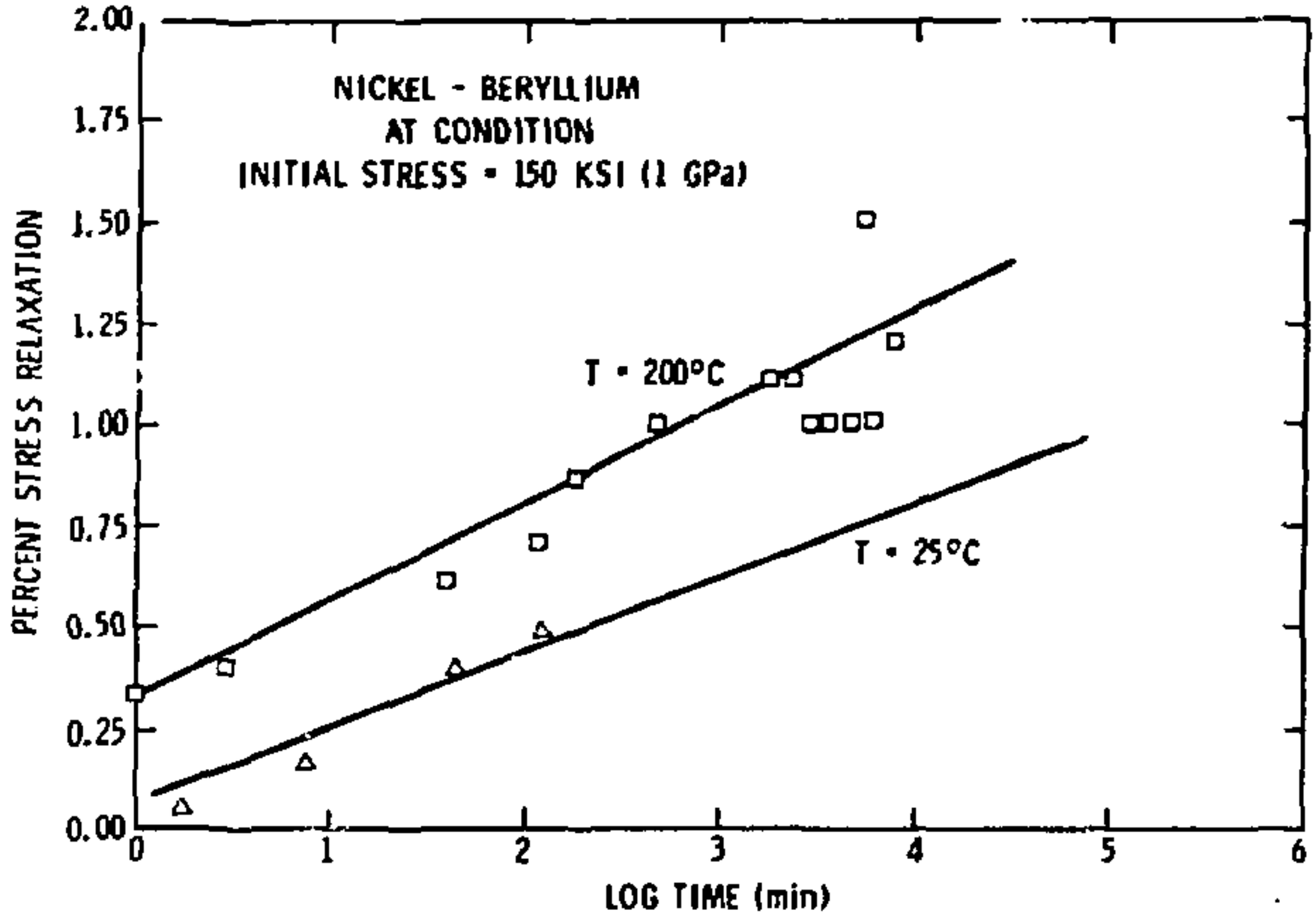

Figure 11: Temperature dependence of the stress relaxation behavior of beryllium-nickel alloy 440, condition AT.

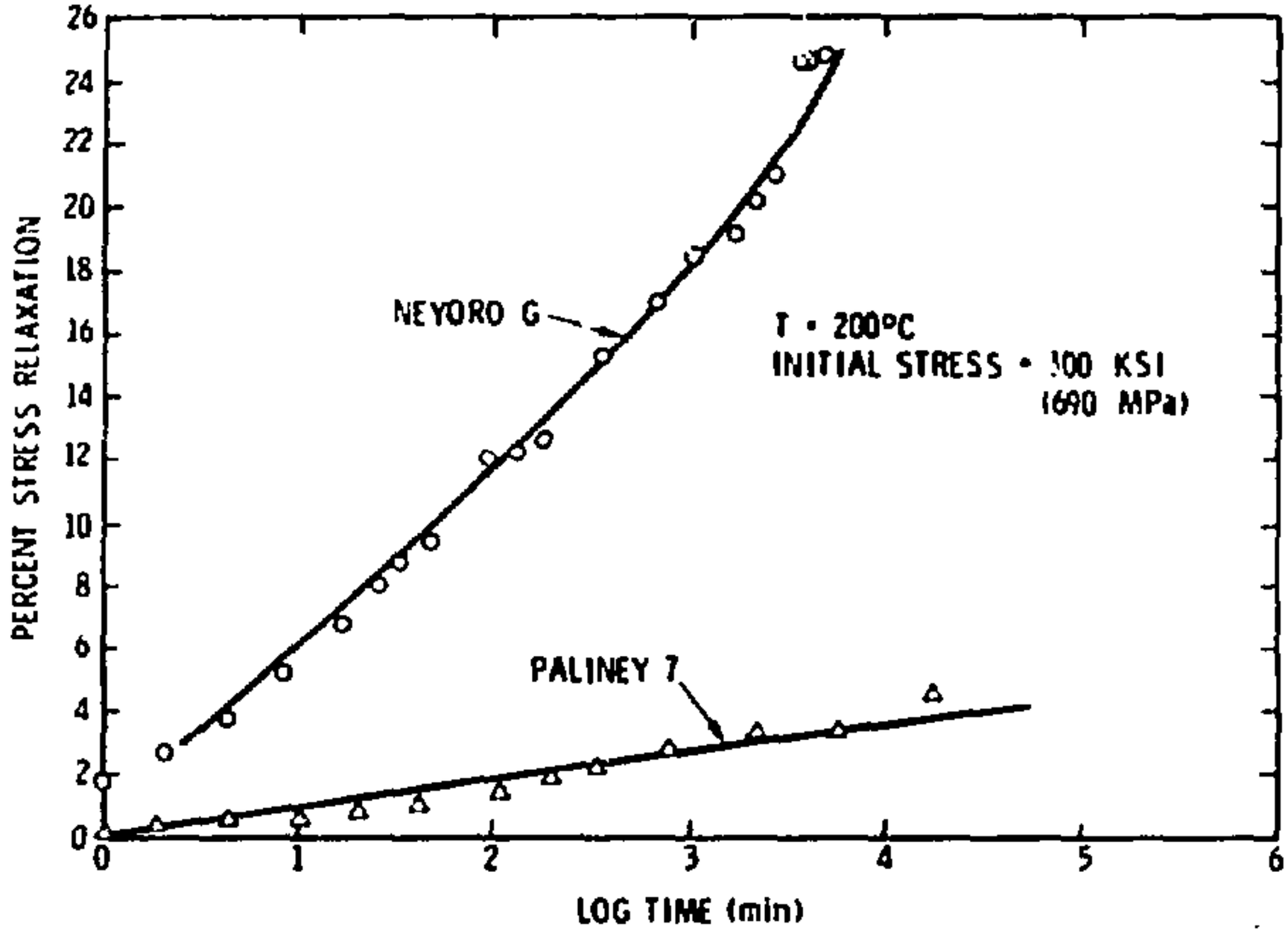

Figure 12: Elevated temperature stress relaxation behavior Paliney 7 and Neyoro G. Initial condition of samples same as outlined in Figures 9 and 10.

recovery mechanisms are beginning to be an important part of the deformation process. The low temperature deformation model presented earlier which contains only work-hardening and no recovery is then no longer valid. Data from the Hey Company give indication of similar behavior,[11] though their results show Neyoro G relaxing to even greater extents than found here. They appear to have used samples that had undergone a different heat treatment than the standard heat treatment which we employed. Based on the results from both studies, it is obvious that Paliney 7 is better than Neyoro G for elevated temperature services. Alloy 440 is clearly superior to both Hey alloys at elevated temperature.

CONCLUSIONS

The following conclusions can be drawn from the results:

1) From a mechanical properties standpoint, beryllium-nickel alloy 440 is equal or superior to the normally used Neyoro G and Paliney 7 for electrical spring contact applications under normal Sandia requirements.

2) For elevated temperature applications, the mechanical properties of beryllium-nickel alloy 440 are clearly superior. Paliney 7 is superior to Neyoro G.

3) There is a measurable difference in heat treating kinetics for the microyield and macroyield behavior in the beryllium-nickel. The magnitude of the difference is small so that for practical purposes batch to batch variations in a normal heat treat operation would mask the effects. Thus, the aging of alloy 440 for times and temperatures other than manufacturers recommendations is unnecessary.

4) Macrodeformation behavior does appear to be a reasonable predictor of the more difficulty measured microdeformation behavior which is important for spring contact materials.

5) A model was presented based on sound physical descriptions of the processes involved in stress relaxation which correctly predicts the time dependence of stress relaxation at room temperature. This allows extrapolation of our relatively short term tests to predict the long term behavior of the alloys when stored in a stressed state.

ACKNOWLEDGMENTS

W. J. Koone assisted with the mechanical testing program. The transmission electron microscopy work of C. R. Hills and the scanning microscopy work of S. F. Iuliere are also acknowledged. The critical comments of the reviewers J. C. Swearengen II and J. A. Van Den Avyle were most useful.

REFERENCES

1. [illegible] and I. W. Tipping, "On Choosing Spring Materials for the Electrical Contacts in the MC 2897 Deceleration Switch," [illegible]

2. [illegible] and I. W. Tipping, "An Evaluation of Three Commercial Grade Nickel Alloys for Electrical Contacts in a Deceleration Switch," [illegible], February 1974.

3. "Beryllium Nickel Alloy 440 Product Data," File Number 3062-PDIA, Hawaiki-Beryllco Industries, New York.

4. "Hey Precious Metal Contacts," J. M. Hey Company, Bloomfield, Conn.

5. [illegible] "Viscoplastic Behavior of Several Precious Metal Electrical Contact Alloys," IEEE Trans. on Parts, Hybrids and Packaging, PHP-11, 29, March 1975.

6. T. V. Nordstrom and R. W. Rohde, "Mechanical Properties and Stress Relaxation of Beryllium-Copper 25," SC-DR-720471, August 1972.

7. Baer, Hans Gunter and Pfeiffer, C. 7., Metallkunde, 64, 740 (1973).

8. J. Wertman, "Mechanical Properties II," Physical Metallurgy ed. by R. W. Cahn, 989 (1974) American Elsevier, New York.

9. R. W. Rohde and T. V. Nordstrom, "Stress Relaxation of a Copper-1.97 wt.% Beryllium Alloy," Material Science and Engineering, 12, 179 (1973).

10. T. V. Nordstrom and R. W. Rohde, "Mechanical Properties and Stress Relaxation of Beryllium-Copper 25," SC-DR-720471.

11. "Elevated Temperature Relaxation of Hey Alloys," Technical Bulletin A-68, J. M. Hey Company, Bloomfield, Conn.